

1 Spatio-temporal dynamics of bluefin tuna (*Thunnus thynnus*) in US waters of the
2 northwest Atlantic

3 Alexander Hansell¹, Sarah Becker², Steven X. Cadrin³, Matt Lauretta⁴, John Walter⁴, Lisa Kerr²

4 1) Northeast Fishery Science Center, NOAA, Woods Hole, MA, USA

5 2) Gulf of Maine Research Institute, Portland, ME, USA

6 3) School for Marine Science and Technology, University of Massachusetts Dartmouth, New
7 Bedford, MA, USA.

8 4) Southeast Fishery Science Center, NOAA, Miami, Florida, USA

9
10 **Abstract**

11 Atlantic bluefin tuna (*Thunnus thynnus*) are large, highly migratory fish that support important fisheries.
12 Oceanic conditions influence Atlantic bluefin tuna distribution and it has been hypothesized that stock
13 distributions have shifted in recent years. Distributional shifts can affect regional availability and fleet
14 catchability, introducing a potential bias in fisheries dependent data used for indexing population
15 trends. We developed a vector auto-regressive spatio-temporal model (VAST) to estimate changes in
16 bluefin tuna spatial distribution in US waters and created standardized indices of abundance for large (>
17 177 cm) and small size classes (≤ 177 cm) of fish. Local-scale environmental factors (sea surface
18 temperature (SST), ocean depth) and regional-scale drivers (e.g., Atlantic Multidecadal Oscillation (AMO)
19 and prey biomass) of spatial distribution were explored. Results indicated that from 1993 to 2020,
20 spatial distribution of the larger size class was highly variable, but on average, the total estimated area
21 occupied increased by 96 km²/year and the center of gravity shifted 2 km/year north and 3 km/year
22 east. Results were similar for the smaller size class fish with an average increase in area occupied of 71
23 km²/year. The center of gravity shifted an average of 1 km/year north and 2 km/year east. The primary
24 factor driving the spatial shifts for both large and small fish was local-scale SST. Standardized indices of
25 abundance were produced and incorporated SST as a covariate of local density. In comparison to prior
26 standardization results, spatio-temporal indices demonstrated less inter-annual variability and produced
27 similar overall trends. This study advanced our understanding of bluefin tuna spatial distributions and
28 generated indices of relative abundance in US waters of the Northwest Atlantic that are more robust to
29 spatio-temporal changes in tuna distributions for consideration in future stock assessments.

30

31 **Introduction**

32 Atlantic bluefin tuna (*Thunnus thynnus*) are highly migratory fish with complex spatial and temporal
33 distribution patterns. Their fisheries are assessed and managed as two distinct stocks (eastern and
34 western) by the International Commission for the Conservation of Atlantic Tunas (ICCAT) with the
35 management boundary at the 45° west meridian (ICCAT 2017, 2020; Kerr et al. 2020). For the western
36 stock, conventional and electronic tagging data showed wide-ranging movements of bluefin tuna
37 between feeding and spawning areas, with seasonal migrations observed between the northern U.S.
38 and Canada to the Gulf of Mexico and back (Galuardi et al. 2010). In addition, extensive mixing of fish
39 across the management boundary was documented (Block et al. 2005, Boustany et al. 2008), supported
40 by evidence of catches in the West Atlantic fisheries containing large proportions of eastern Atlantic
41 origin fish (Kerr et al. 2020). Further, ocean climate is known to be an important determinant of the
42 distribution and dynamics of bluefin tuna (Humston et al. 2000, Schick et al. 2004, Golet et al. 2013,
43 Druon et al. 2016) with substantial shifts in the spatial distribution of bluefin tuna being documented in
44 response to changing ocean conditions (e.g., Golet et al. 2013, Fromentin et al. 2014, MacKenzie et al.
45 2014, Druon et al. 2016).

46 U.S. fisheries for Atlantic bluefin tuna operate in the northwest Atlantic, a productive foraging region for
47 bluefin tuna. Substantial changes in oceanographic conditions have occurred in the region over the last
48 two decades, including an increase in sea surface temperature at a rate that faster than most regions of
49 the world's ocean (SST; Pershing et al., 2018). Coincident with these changes in fish habitat, are well
50 documented poleward shifts in marine taxa distributions (Nye et al., 2009; Pinsky et al., 2013). It is
51 hypothesized that similar spatial distribution shifts have occurred for bluefin tuna; however, the exact
52 extent and drivers of bluefin tuna spatial distribution remain unknown (Walter, 2018). For other species,
53 distribution shifts in the region have been attributed to local environmental variables (SST and depth);
54 regional drivers (e.g., length of summer; Henderson et al. 2017); basin wide climate indices (e.g., AMO;
55 Nye et al., 2009); prey distribution (Golet et al., 2013) and fishing effects (Adams et al., 2018). To identify
56 the primary causes of distributional change, it is important that potential drivers are evaluated using a
57 consistent framework, so that estimation models can accurately quantify the effect and variation
58 attributed to the various factors (Thorson et al., 2017; Perretti and Thorson, 2019).

59 In the West Atlantic region, the recent stock assessments of bluefin tuna relied on two analytical models
60 (i.e., Virtual Population Analysis and Stock Synthesis) that were fit to fishery dependent indices of
61 abundance in the form of flag and fleet-specific catch-per-unit-effort (CPUE) time series (ICCAT, 2020).

62 The assessments were challenged by the need to resolve conflicting trends between U.S. and Canadian
63 CPUE indices (ICCAT, 2017). Researchers hypothesized that conflicting trends resulted from bluefin tuna
64 shifting northward away from U.S. fishing areas toward Canadian waters as a result of changing ocean
65 conditions (Walter, 2018). Shifting spatial distributions can complicate the interpretation of data used in
66 the stock assessment due to systematic change in fish availability to regional fishing fleets (i.e., time-
67 varying catchability). The change in availability could be misinterpreted as a stock decline in regions
68 where the fish have migrated away from, or stock abundance increase in the regions with increased fish
69 availability or density (Wilberg et al. 2010, Link et al 2011). Stock assessment analysts explored several
70 approaches to reconcile conflicting trends, and ultimately decided to incorporate the influence of an
71 environmental covariate (i.e., Atlantic Multidecadal Oscillation) on catchability for U.S. and Canadian
72 handline indices using Stock Synthesis. In contrast, the assessment team removed the U.S. and Canadian
73 commercial handline indices from the Virtual Population Analysis, as divergent trends in the commercial
74 fisheries could not be reconciled within the model (ICCAT 2020).

75 Currently, two standardized indices are produced from the U.S. handline (i.e., rod and reel) fisheries;
76 one indexing smaller tuna (66-144 cm) caught by the recreational fishery and a second index of
77 commercially-sold, large-sized fish (>177 cm). Standardization models applied to the fishery dependent
78 data did not explicitly account for spatio-temporal changes, but attempted to account for spatial
79 changes associated with thermal habitat characteristics by modeling SST as a covariate of fleet
80 catchability (Hansell et al., 2021a; Laretta et al., 2021). A potential problem with the approach is that
81 SST may affect localized fish density or abundance, and if so, the approach may mask a trend in
82 abundance and attribute the change in CPUE as a catchability effect.

83 Here, we applied a vector auto-regressive spatio-temporal model (VAST) to produce indices of Atlantic
84 bluefin tuna relative abundance in U.S. waters for two size classes, large commercially-sized (> 177cm)
85 and small tuna caught by the recreational fishing fleet (≤ 177 cm). We evaluated the extent to which
86 spatial shifts in bluefin tuna distribution occurred, and whether these shifts can be attributed to local or
87 regional oceanographic factors, or prey abundance. The influence of different environmental covariates
88 was assessed to determine the effects of changes in fleet catchability versus local density. The results
89 provided new insight into bluefin tuna spatial distribution in U.S. fishing areas and produced two indices
90 of relative abundance that are expected to be more robust to spatio-temporal drivers of both fish
91 availability and fleet catchability. We recommend that future stock assessments take into account these
92 data improvements, as the CPUE series provide essential data on fishery and stock trends.

93 **Methods**

94 **Fishery Data**

95 The U.S. Large Pelagics Survey is a dockside survey of private vessel and charter boat captains who have
96 just completed fishing trips directed at large pelagic species (Foster et al. 2008). The survey is conducted
97 at public fishing access sites that are likely to be used by offshore anglers, and was primarily designed to
98 collect detailed catch and effort data. For this study, analyses focused on trips that targeted bluefin with
99 rod and reel from June to October and spent less than 24 hours fishing because this is when the majority
100 of fishing occurs (Figure 1). Information collected by the survey included: date, fishing location (lat/lon),
101 number of fishing lines in the water, hours fished, and catch by size category (Lauretta et al 2020; Table
102 1). Past CPUE standardizations did not incorporate young school (< 66 cm SFL) and small medium size
103 classes (145-177 cm SFL). However, in this study all sizes of bluefin tuna were included in model
104 development. For all model runs, bluefin tuna were aggregated into two size categories: 1) small (≤ 177
105 cm) and 2) large (> 177 cm).

106 **Spatio-temporal model**

107 VAST is a delta-model that separates catch into two components: 1) the probability of a positive catch,
108 and 2) the positive catch rate. The probability of a positive catch observation was estimated using a
109 logit-linked linear predictor. Several alternative probability distributions were explored for the second
110 component that modeled the catch rate on positive (at least one bluefin tuna was caught) fishing trips,
111 including Poisson, negative binomial, gamma, log-normal models.

112 Probability of a bluefin tuna observation:

113
$$\text{logit}^{-1}(P_{1,i}) = \beta_1(t_i, c_i) + \omega_1(s_i, c_i) + \varepsilon_1(s_i, c_i, t_i) + \sum_{j=1}^{n_j} \lambda_1(j, c_i)x(j, s_i, t_i)Q(i, k_1)$$

114 Bluefin tuna catch rate on positive trips:

115
$$\text{log}(P_{2,i}) = \beta_2(t_i, c_i) + \omega_2(s_i, c_i) + \varepsilon_2(s_i, c_i, t_i) + \sum_{j=1}^{n_j} \lambda_2(j, c_i)x(j, s_i, t_i)Q(i, k_2)$$

116 Where P_1 is the probability of positive catch, P_2 is the probability of the catch given the catch is positive,

117 $\beta(t_i)$ is the intercept for each year t and length-group c and is modeled as a random walk, $\omega(s_i)$ is a
 118 time-invariant spatial autocorrelated variation for knot s and length-group c , $\varepsilon(s_i, c_i, t_i)$ is a time-varying
 119 spatial-temporal autocorrelated variation for knot s and length-group c in year t , $\lambda(j, c_i)$ is the effect of
 120 covariate j on length group c , n_j is the number of covariates and $x(j, s_i, t_i)$ is the value of covariate j in
 121 knot s in year t , $Q(i, k)$ is the fixed effect estimates for catchability, and the integer subscripts denote
 122 the model component (1: presence/absence, 2: non-zero density) for observation i .

123 The spatial processes ($\omega_1(s_i, c_i)$; $\omega_2(s_i, c_i)$) were modeled as Gaussian Markov random fields with
 124 correlation over two spatial dimensions and among fish size (e.g., ≤ 177 or > 177 cm).

$$125 \quad \text{vec}(\Omega_p) \sim \text{GRF}(0, R_p \otimes V_{wp})$$

126 Where Ω_p is a matrix composed of $\omega_2(s_i, c_i)$ at every knot s and length bin c , R_p is correlation between
 127 knots, and V_{wp} is correlation between length bins.

$$128 \quad V_{wp} = L_{wp} L_{wp}^T$$

129 Where L_{wp} is a matrix representing covariance among length bins. The spatial covariance between
 130 knots s and s^* was modeled as a Matern process.

$$131 \quad R_p(s, s^*) = \frac{1}{2^{v-1} \Gamma(v)} (K_p H |s - s^*|)^v K_v(K_p H |s - s^*|)$$

132 Where v is a smoothness parameter that is fixed at 1, K_p controls the distance correlation and reduces
 133 to zero, K_v is a Bessel function and H is a two dimensional anisotropic distance function. The spatio-
 134 temporal processes ($\varepsilon_{1,2}(s_i, c_i, t_i)$) were fit independently for each year, and were modeled with
 135 Gaussian Markov random fields assuming a Matern covariance.

136 In addition to catchability covariate effects, estimated values of the fixed and random effects predicted
 137 local density ($d(s, t)$) for knot s and length-group c in year t .

$$138 \quad d(s, t) = \text{logit}^{-1} \left(\beta_1(t_i, c_i) + \omega_1(s_i, c_i) + \varepsilon_1(s_i, c_i, t_i) \right) \times \exp \left(\beta_2(t_i, c_i) + \omega_2(s_i, c_i) + \varepsilon_2(s_i, c_i, t_i) \right)$$

139

140 The index of abundance ($B(t)$) is calculated as the sum of the density of each knot using an area
 141 weighted approach:

142

$$B(t) = \sum_{s=1}^{n_s} (a(s) \times d(s, t))$$

143

144

145

146

147

148

Where $B(t)$ is the area weighted density for each knot in year t throughout the specific domain, which in this study is Virginia to Maine and $a(s)$ is the area of knot s . A mesh approach (200 knots) which allows for anisotropy was used to fit the model. Parameter estimation used Template Model Builder (Kristensen et al. 2016) and the R program (R Core Team 2020). Model convergence was examined by ensuring the maximum gradient of the likelihood estimation was less than 0.0001 for all parameters and the Hessian matrix was positive definite.

149

Explanatory covariates

150

151

152

153

154

155

156

157

158

159

160

161

162

163

164

165

We explored local and regional covariates as drivers of catchability and density. Local covariates varied across space, while regional covariates were univariate and represented temporal changes affecting the stock. Number of fishing lines were explored as an influence on catchability, while local covariates, month, SST and depth were explored as drivers of catchability or density (Figure 2). Bathymetry data acquired from the *marmap* package in R (Pante and Simon-Bouchet, 2013) was used to estimate depth at each fishing location, while satellite-derived estimates of weekly mean SST were matched to each fishing event on a one-degree latitude by one-degree longitude scale (NOAA 2021a). All local covariates were fit with polynomial splines to allow for non-linear relationships, which are common in ecological data. The optimal number of knots used to fit each polynomial spline was determined automatically by the *Splines2* package in R, which accounts for degrees of freedom and the quantiles of the explanatory covariates (Wang 2021). Regional covariates were estimated as annual time series and included annual deviations in SST and prey abundance (Figure 3). Deviations in SST were estimated as the AMO index, matching the time series used in the last western bluefin tuna stock assessment, applied to large fish index analysis (ICCAT, 2020; Hansell et al. 2020). In characterizing prey abundance, we focused on a key prey of bluefin tuna, Atlantic herring. Atlantic herring biomass and estimates were obtained from the 2020 Atlantic herring stock assessment (Golet et al. 2013; NOAA, 2021b).

166

167

168

169

170

In VAST, estimated spatial random fields were expected to account for the changes in distribution over the time series and capture residual patterns that cannot be attributed to fixed effects (explanatory covariates). Thus, we used the approach to determine the importance of each variable in potential distribution shifts by setting the spatial effects of the model to zero and generating a time series of center-of-gravity estimates. The center-of-gravity estimates from the model without the random fields

171 were then compared to the model with random fields to determine the amount of variation caused by
172 each covariate; this process is referred to as counterfactual analysis (Pearl, 2009; Perretti and Thorson,
173 2019). Collinearity of covariates was examined using generalized variance-inflation factor (GVIF) scores.
174 Any covariate with a score greater than three was removed, and the GVIFs were recalculated (Zuur, et
175 al. 2012). For CPUE standardization, Akaike Information Criterion (AIC) scores were used to determine
176 the best-fitting model. If AIC scores were within two units of one another, the most parsimonious model
177 was selected (Burnham and Anderson, 2004). AIC was used to determine if a covariate improved model
178 information content as an index for catchability versus density.

179 **Results**

180 CPUE was measured as the number of fish caught per hour (catch/hour; Table S1). A gamma probability
181 function was selected to model the distribution of positive catch rates. All models using CPUE and
182 gamma distributions converged and diagnostics suggested no major issues with model performance
183 occurred. SST and month were collinear; therefore, month was excluded from model runs (Figure S1 –
184 S4; Table S2 & S3).

185 A model fit with all local and regional environmental covariates suggested that from 1993 to 2020, large
186 fish spatial distributions varied notably; however, on average, the area of occupancy increased by 96.4
187 km²/year, and the center of gravity shifted north and east at an average rate of 2.3 km/year and 3
188 km/year (Figure 4;6-7). We observed similar patterns for small fish distributions with the area of
189 occupancy increasing on average 70.6 km²/year, and the center of gravity shifting north and east at an
190 average rate of 1.1 km/year and 1.7 km/year (Figure 5-7). Counterfactual analysis suggested that the
191 covariates in the model accounted for the majority of observed spatial distribution deviations (Figure 8).
192 Sensitivity runs suggested that SST was the primary driver of observed spatial distribution shifts, with
193 depth, AMO, and herring abundance having considerably less influence (Figure 9).

194 The best-fit model, as determined by AIC, included SST as a covariate for density (Table 2). Estimated
195 indices of bluefin tuna abundance, from the best fit model, showed variability throughout the time
196 series for both large and small size classes; however, an increased trend in the large fish index was clear
197 after 2013 (Figure 10). Compared to the conventional index, the large fish index from VAST produced a
198 lower abundance estimate in the 1990's and early 2000's while producing higher estimates from 2004 to
199 2010. The small fish index from VAST produced lower abundance estimates at the beginning and end of
200 the time series (Figure 10).

201 **Discussion:**

202 The VAST model provided a single integrated spatio-temporal framework to examine the spatial
203 distribution changes of bluefin tuna and estimate indices of relative abundance by size. VAST estimated
204 that the area of occupancy increased over the entire time period and the center of gravity shifted
205 northeast for both large and small bluefin. These results confirm previous hypotheses that the
206 population of bluefin tuna has shifted northward away from U.S. fishing areas towards Canadian waters
207 (Walter et al. 2018; Hansell et al. 2020).

208 Understanding the underlying mechanisms of tuna spatial distributions is essential to account for
209 changes in fish availability, particularly in terms of fisheries management and fleet catch allocations
210 (Link et al. 2011). In this study, the primary driver of bluefin tuna distribution was local SST, which may
211 have multiple influences on Atlantic bluefin tuna and their prey (Table 2; Figure 9). Previous work has
212 demonstrated the importance SST plays in bluefin tuna habitat/distribution. Thus, it was not surprising
213 our analyses estimated SST as an important driver of bluefin tuna spatial distribution (Teo et al. 2007;
214 Schick et al. 2004; Golet et al 2013). Additionally, the North Atlantic has experienced substantial
215 increases in SST in recent years and these increases have been linked to the northward shift of many
216 taxa in the region (Nye et al. 2009; Pinsky et al. 2013). Our results corroborate those observed patterns
217 for Atlantic bluefin tuna.

218 We expected herring abundance or the AMO index to have more of an effect on bluefin tuna
219 distribution estimates, given previous work showing that both of these covariates are important in
220 bluefin tuna distribution (Golet et al. 2013; Faillettaz et al. 2019). For herring, differences in this study
221 could be the result of scale, because past studies have examined fine scale data while this study
222 examined data at an annual time step (Golet et al. 2013). The lack of influence of the AMO in this study
223 could be due to the short time series of data (1993-2020) evaluated. During this time period, the AMO
224 was in a consistent warm phase (Figure 3). Additionally, in fitting the AMO as a climate indicator in the
225 stock assessment, it was estimated to have a stronger relationship with Canadian indices than US
226 indices. The differential effect on northern areas may be a factor contributing to a lack of estimated
227 effect in the U.S. fishing areas (Hansell et al., 2020). Despite identifying the primary driver of spatial
228 distribution change (SST) it is possible other environmental drivers (e.g., Atlantic Meridional Overturning
229 Circulation), or prey species could be influencing bluefin distribution. Especially since bluefin tuna have

230 complex migration patterns, are top predators with a diverse diet and the data in this study only focuses
231 on a short seasonal window (June – October) when the fish are available to the fishery.

232 In the U.S., a reliable fisheries independent survey is not available for bluefin tuna and thus, this study
233 relied on fisheries dependent data. In the absence of surveys, fisheries data is commonly used as an
234 input to stock assessment; however, fishing locations are not chosen at random (Maunder and Punt,
235 2004). Thus, it was difficult to determine if spatial distribution shifts were related to changes in fish
236 distribution or changes in fishing behavior.

237 Our results suggest that abundance of small fish in the area was highly variable from one year to the
238 next, but abundance of large fish increased in recent years. These findings are consistent with previously
239 developed indices of abundance for bluefin tuna (Figure 10). Results also supported previous
240 hypotheses that spatial distribution changes have occurred in both the population and the fishery
241 (Walter, 2018; Figures 4-7), validating the use of a spatio-temporal model for CPUE standardization. The
242 use of spatio-temporal approach is further validated due to low captures (< 100 fish), in the Large Pelgics
243 Survey, in certain years (Table S1). VAST can handle low sample sizes and provide estimates for missing
244 covariates (Thorson, 2019); however, despite this ability model results for these years (2003, 2006,
245 2008, 2014) are probably more uncertain and should be viewed with caution.

246 The VAST model presented here improved upon previous conventional CPUE standardization
247 approaches that modeled size classes separately and accounted for spatial changes by incorporating SST
248 (Hansell et al., 2021; Laretta et al., 2021). The time series of abundance produced from VAST were
249 similar to previous methods; however, there were some differences in the large fish index in the early
250 2000 and the small fish index near the end of the time series (Figure 10). Potential differences in relative
251 abundance were not necessarily the result of model structure but could be the result of data decisions.
252 For example, past indices of abundance used captures as the explanatory variable and effort as an
253 offset, while the VAST model used CPUE (catch/hours). Typically, it is not appropriate to use hours in the
254 denominator of CPUE because it assumes each hour of fishing has the same probability of catching a fish
255 (Peterson et al., 2017). However, we believe this is not a substantial problem here because all fishing
256 trips used were relatively short (< 24 hours). The index applies to the rod and reel fishery where bait was
257 constantly checked, and fishermen chum to attract fish. Another difference between the VAST model
258 and past standardizations was that two additional size classes are included in the model for small fish (<

259 66 cm and 145-177 cm; Table 1). Lastly, the large fish index used all trips from Virginia to Maine, while
260 the previous model focused solely on trips in the Gulf of Maine (Hansell et al., 2020).

261 We recommend that future assessments should explore incorporating the indices produced here into
262 the stock assessment because geo-statistical approaches like VAST are expected to yield more accurate
263 indices of abundance (Shelton et al. 2014). Additionally, using these models in assessments may lead to
264 lower retrospective bias (a notable problem identified during the last stock assessment, particularly the
265 VPA), and potentially provide more accurate biomass estimates compared to design based index-driven
266 models (Cao et al. 2017). Further, VAST supported the use of local SST as being an important driver of
267 density and distribution changes; however, current standardization models incorporate SST as a
268 covariate of catchability. Thus, current approaches may be detrending the effect of SST, which could
269 alter year effect estimates. We anticipate this approach will continue to be useful as sea temperatures in
270 the Northeast U.S. are projected to continue to increase at three times the global rate of change (Saba
271 et al. 2016).

272 Future work should also explore combining the results presented here with commercial fisheries data in
273 Canada. Combining data into a joint index would create a single time series that could resolve residual
274 patterns between the two fleets (Hansell et al., 2020). A similar approach of a combined index was
275 applied to U.S. and Mexican longline fisheries that target bluefin tuna in the Gulf of Mexico (Lauretta et
276 al., 2021). Previously, a joint index between U.S. and Canadian fisheries was explored by the ICCAT Index
277 Working Group; however, it was not recommended due to differences in catch distribution between the
278 countries (Hansell et al., 2021). VAST can potentially reconcile this issue because it has the ability to
279 combine multiple data types into an integrated modeling framework (Gruss et al., 2019). Additionally,
280 adding the Canadian data into VAST could allow for the exploration of larger-scale distribution shifts and
281 potential drivers of bluefin tuna habitat that are more reflective of the population as a whole.

282 In conclusion, the VAST model provided a single framework to estimate distribution changes and indices
283 of bluefin tuna relative abundance in US waters. The model estimated that for both large and small fish,
284 the area occupied increased, and the center of gravity shifted northeast. Our results highlighted local
285 SST as a primary driver of the estimated spatial shifts. Compared to conventional standardization
286 models, spatio-temporal indices showed less inter-annual variability between year effects, but produced
287 similar overall trends. Results are expected to increase the understanding of bluefin tuna spatial
288 distribution in U.S. waters and produce indices that are more robust to spatio-temporal changes. The

289 findings have implications for the management of bluefin tuna in terms of stock status determinations
290 and sustainable catch forecasts, and we recommend that the indices produced be directly incorporated
291 into future stock assessments.

292 **Acknowledgments:**

293 We would like to thank the Kerr lab at the Gulf of Maine Research Institute as well as the ICCAT Index
294 working group for feedback on early drafts of the model. Special thanks to Alex Hanke, Brooke Lowman
295 and Andrew Allyn who helped with model development. We appreciate the feedback from anonymous
296 reviewers. Funding for this project was provided by the U.S. NOAA Bluefin Tuna Research Program
297 (NA19NMF4720096). The scientific results and conclusions, as well as any views or opinions expressed
298 herein, are those of the authors and do not necessarily reflect those of their institutions.

299 **References:**

- 300 Adams, C.F., Alade, L.A., Legault, C.M., O'Brien, L., Palmer, M.C., Sosebee, K.A., Traver, M.L., 259 2018.
301 Relative importance of population size, fishing pressure and temperature 260 on the spatial distribution
302 of nine Northwest Atlantic groundfish stocks. PLOS ONE 13, e0196583.
303 <https://doi.org/10.1371/journal.pone.0196583>
- 304 Block, B.A., Teo, S., Walli, A., Boustany, A., and Stokesbury, M.J.W., Farwell, C.J., Weng, K.C., Dewar, H.,
305 and Williams, T.D. 2005. Electronic tagging and population structure of Atlantic bluefin tuna. *Nature*
306 434: 1121–1123. doi:10.1038/nature03463.
- 307 Boustany, A.M., Reeb, C.A., and Block, B.A. 2008. Mitochondrial DNA and electronic tracking reveal
308 population structure of Atlantic bluefin tuna (*Thunnus thynnus*). *Mar. Biol.* 156(1): 13–24.
- 309 Burnham, K. P., & Anderson, D. R. (2004). Multimodel inference: understanding AIC and BIC in model
310 selection. *Sociological methods & research*, 33(2), 261-304.
- 311 Cao, J., Thorson, J. T., Richards, R. A., & Chen, Y. (2017). Spatiotemporal index standardization improves
312 the stock assessment of northern shrimp in the Gulf of Maine. *Canadian Journal of Fisheries and Aquatic*
313 *Sciences*, 74(11), 1781-1793.
- 314 Druon, J.-N., Fromentin, J-M, Hanke, A.R., Arrizabalaga, H., Damalas, D. et al. 2016. Habitat suitability of
315 the Atlantic bluefin tuna by size class: An ecological niche approach. *Progr. Oceanogr.* 142: 30–46.
- 316 Foster, J., R. Salz, T. R. Sminkey, D. Van Voorhees, R. Andrews, and H.-L. Lai. 2008. Large pelagic survey:
317 methodology overview and issues. ICES CM 2008/K:22.

318 Fromentin, J-M., Reygondeau, G., Bonhommeau, S., and Beaugrand, G. 2014. Oceanographic changes
319 and exploitation drive the spatio-temporal dynamics of Atlantic bluefin tuna (*Thunnus thynnus*). Fish.
320 Oceanogr. 23(2):147-156.

321 Galuardi, B., Royer, F., Golet, W., Logan, J., Neilson, J., & Lutcavage, M. (2010). Complex migration routes
322 of Atlantic bluefin tuna (*Thunnus thynnus*) question current population structure paradigm. *Canadian*
323 *Journal of Fisheries and Aquatic Sciences*, 67(6), 966-976.

324 Golet, W.J., Galuardi, B., Cooper, A.B., and Lutcavage, M.E. 2013. Changes in the distribution of Atlantic
325 bluefin tuna (*Thunnus thynnus*) in the Gulf of Maine 1979-2005. PLoS ONE 8(9): e75480.
326 doi:10.1371/journal.pone.0075480

327 Grüss, A. and Thorson, J.T. (2019) Developing spatio-temporal models using multiple data types for
328 evaluating population trends and habitat usage. *ICES Journal of Marine Science* 76, 1748–1761.
329 doi:10.1093/icesjms/fsz075.

330 Hansell, A., Becker S., Brown, C., Cadrin, S., Golet, W., Laretta, M., Walter, J., Kerr, L. 2021a.
331 INVESTIGATION OF MODEL IMPROVEMENTS FOR THE U.S. ROD AND REEL LARGE (>177 cm) ATLANTIC
332 BLUEFIN TUNA INDEX OF ABUNDANCE. SCRS/2021/038
333

334 Hansell, A., Walter, J., Cadrin, S., Golet, W., Hanke, A., Laretta, M., & Kerr, L. (2020). INCORPORATING
335 THE ATLANTIC MULTIDECADAL OSCILLATION INTO THE WESTERN ATLANTIC BLUEFIN TUNA STOCK
336 ASSESSMENT. *Collect. Vol. Sci. Pap. ICCAT*, 77(2), 376-388.

337 Hansell A., Hanke A., Becker, S., Cadrin S., Laretta M., Walter, J., Golet, W., and Kerr L. 2021b.
338 Development of a wester large (>177 cm) Atlantic bluefin tuna index of abundance based on Canadian
339 and US Rod and Reel Fisheries Data. SCRS Technical Work Group on Indices. Online March 26th, 2021.

340 Henderson, M.E., Mills, K.E., Thomas, A.C., Pershing, A.J., Nye, J.A., 2017. Effects of spring 287 onset and
341 summer duration on fish species distribution and biomass along the 288 Northeast United States
342 continental shelf. *Rev. Fish Biol. Fish.* 27, 411–424. 289 <https://doi.org/10.1007/s11160-017-9487-9>

343 Humston, R., Ault, J.S., Lutcavage, M., and Olson, D.B. 2000. Schooling and migration of large pelagic
344 fishes relative to environmental cues. *Fish. Oceanogr.* 9:136-146.

345 ICCAT. 2017a. Report of the 2017 Atlantic bluefin tuna stock assessment session (Madrid, Spain –
346 September 22 to 27, 2017).

347 ICCAT. 2020. Report of the 2020 Atlantic bluefin tuna stock assessment session (Madrid, Spain –
348 September 22 to 27, 2020).

349 Kristensen, K., Nielsen, A., Berg, C., Skaug, H., Bell, B., (2016). TMB: Automatic Differentiation and
350 Laplace Approximation. *Journal of Statistical Software*, 70(5), 1-21. doi:10.18637/jss.v070.i05

351 Kerr, L. A., Whitener, Z. T., Cadrin, S. X., Morse, M. R., Secor, D. H., & Golet, W. (2020). Mixed stock
352 origin of Atlantic bluefin tuna in the US rod and reel fishery (Gulf of Maine) and implications for fisheries
353 management. *Fisheries Research*, 224, 105461.

354 Link, J.S., Nye, J.A., Hare, J.A. 2011. Guidelines for incorporating fish distribution shifts into a fisheries
355 management context. *Fish Fish.* 12:461-469.

356 Lauretta, M. Walter J., and Brown C. 2021. The United States rod and reel smaller sizeclass bluefin tuna
357 (*Thunnus thynnus*) indices of relative abundance; major revisions and recommendations. SCRS/2021/034

358 MacKenzie, B.R., Payne, M.R., Boje, J., Hoyer, J.L., and Siegstad, H. 2014. A cascade of warming brings
359 bluefin tuna to Greenland waters. *Global Change Biol.* 20(8): 2484-2491.

360 NOAA, 2021a. National Oceanic and Atmospheric Administration Physical Science Laboratory sea surface
361 temperature. Available here: <https://psl.noaa.gov/data/gridded/data.noaa.oisst.v2.html> Accessed on:
362 9/15/2021

363 NOAA, 2021. Atlantic herring stock assessment. Available here:
364 [https://www.st.nmfs.noaa.gov/stocksmart?stockname=Atlantic%20herring%20-](https://www.st.nmfs.noaa.gov/stocksmart?stockname=Atlantic%20herring%20-%20Northwestern%20Atlantic%20Coast&stockid=10572)
365 [%20Northwestern%20Atlantic%20Coast&stockid=10572](https://www.st.nmfs.noaa.gov/stocksmart?stockname=Atlantic%20herring%20-%20Northwestern%20Atlantic%20Coast&stockid=10572)

366 Nye, J. A., Link, J. S., Hare, J. A., & Overholtz, W. J. (2009). Changing spatial distribution of fish stocks in
367 relation to climate and population size on the Northeast United States continental shelf. *Marine Ecology*
368 *Progress Series*, 393, 111-129.

369 Pante E, Simon-Bouhet B (2013) marmap: A Package for Importing, Plotting and Analyzing Bathymetric
370 and Topographic Data in R. *PLoS ONE* 8(9): e73051. <https://doi.org/10.1371/journal.pone.0073051>

371 Pearl, J. (2009). Causal inference in statistics: An overview. *Statistics surveys*, 3, 96-146.

372 Peterson, C. D., Gartland, J., & Latour, R. J. (2017). Novel use of hook timers to quantify changing
373 catchability over soak time in longline surveys. *Fisheries Research*, 194, 99-111.

374 Perretti, C. T., & Thorson, J. T. (2019). Spatio-temporal dynamics of summer flounder (*Paralichthys*
375 *dentatus*) on the Northeast US shelf. *Fisheries Research*, 215, 62-68.

376 Pershing, A.J., K.E. Mills, A.M. Dayton, B.S. Franklin, and B.T. Kennedy. 2018. Evidence for adaptation
377 from the 2016 marine heatwave in the Northwest Atlantic Ocean. *Oceanography* 31(2):152–161,
378 <https://doi.org/10.5670/oceanog.2018.213>.

379 Pinsky, M. L., Worm, B., Fogarty, M. J., Sarmiento, J. L., & Levin, S. A. (2013). Marine taxa track local
380 climate velocities. *Science*, 341(6151), 1239-1242.

381 R Core Team (2020). R: A language and environment for statistical computing. R Foundation for
382 Statistical Computing, Vienna, Austria. URL <https://www.R-project.org/>.

383 Saba, V. S., Griffies, S. M., Anderson, W. G., Winton, M., Alexander, M. A., Delworth, T. L., ... & Zhang, R.
384 (2016). Enhanced warming of the Northwest Atlantic Ocean under climate change. *Journal of*
385 *Geophysical Research: Oceans*, 121(1), 118-132.

386 Schick, R.S., Goldstein, J., and Lutcavage, M.E. 2004. Bluefin tuna (*Thunnus thynnus*) distribution in
387 relation to sea surface temperature fronts in the Gulf of Maine (1994-96). *Fish Oceanogr.* 13: 225-238.
388 doi:10.1111/j.1365-2419.2004.00290.x.

389 Shelton, A. O., Thorson, J. T., Ward, E. J., & Feist, B. E. (2014). Spatial semiparametric models improve
390 estimates of species abundance and distribution. *Canadian Journal of Fisheries and Aquatic*
391 *Sciences*, 71(11), 1655-1666.

392 Schick, R. S., Goldstein, J., & Lutcavage, M. E. (2004). Bluefin tuna (*Thunnus thynnus*) distribution in
393 relation to sea surface temperature fronts in the Gulf of Maine (1994–96). *Fisheries*
394 *Oceanography*, 13(4), 225-238.

395 Teo, S. L., Boustany, A. M., & Block, B. A. (2007). Oceanographic preferences of Atlantic bluefin tuna,
396 *Thunnus thynnus*, on their Gulf of Mexico breeding grounds. *Marine Biology*, 152(5), 1105-1119.

397 Thorson, J.T., Barnett, L.A.K., 2017. Comparing estimates of abundance trends and distribution shifts
398 using single- and multispecies models of fishes and biogenic 333 habitat. *ICES J. Mar. Sci.* 74, 1311–1321.
399 <https://doi.org/10.1093/icesjms/fsw193>

400 Thorson, J. T. (2019). Guidance for decisions using the Vector Autoregressive Spatio-Temporal (VAST)
401 package in stock, ecosystem, habitat and climate assessments. *Fisheries Research*, 210, 143-161.

402 Wang W, Yan J (2021). *splines2: Regression Spline Functions and Classes*. R package version
403 0.4.5, <https://CRAN.R-project.org/package=splines2>.

404 Walter, J., Sharma, R., & Ortiz, M. 2018. Western Atlantic bluefin tuna stock assessment 1950-2015
405 using Stock Synthesis. *Collect. Vol. Sci. Pap. ICCAT*, 74(6), 3305-3404.

406 Wilberg, M.J., Thorson, J.T., Linton, B.C., Berkson, J. 2010. Incorporating time-varying catchability into
407 population dynamic stock assessment models. *Rev. Fish. Sci.* 18: 7-24.

408 Zuur, A.F., Saveliev, A.A., Ieno, E.N., 2012. *Zero Inflated Models and Generalized Linear Mixed Models*
409 *with R*. Highland Statistics Ltd, Newburgh

Table 1. Size categories for Atlantic Bluefin tuna defined in the Large Pelagics Survey.

Size Categories	Size
Young school	< 26 in (66cm) SFL
School	26-44 in (66-114 cm) SFL
Large school	45-56 in (115-144 cm) SFL
Small medium	57-69 in (145-177 cm) SFL
Large medium	70-76 in (178-195 cm) SFL
Giant	> 76 in (195 cm) SFL

Table 2. AIC step-wise model selection for VAST catch per unit effort (CPUE) standardization. The table shows the influence of each covariate on model selection. The null model does not include any covariates and delta AIC represents the change each covariate has on overall AIC.

Covariate	Density		Catchability	
	AIC	Δ AIC	AIC	ΔAIC
Null	16489.75			
Number of Lines	-		15977.04	-512.71
SST	15931.1	-558.65	15969.25	-520.5
Depth	16091.89	-397.86	16184.37	-305.38
AMO	16091.89	-397.86	16271.19	-218.56
Herring	16111.23	-378.52	16277.14	-212.61

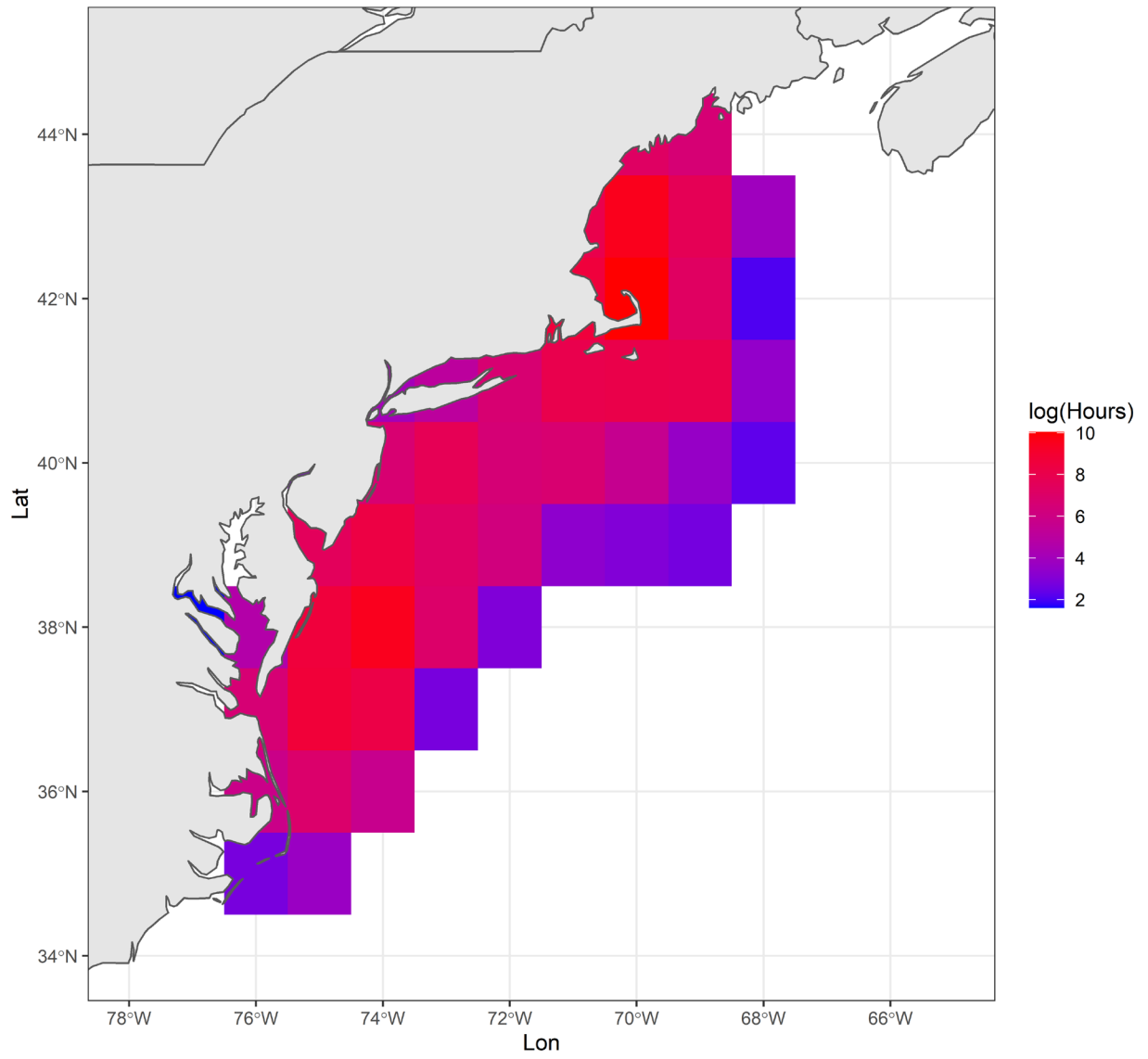


Figure 1. Spatial footprint and number of hours targeting Atlantic bluefin tuna.

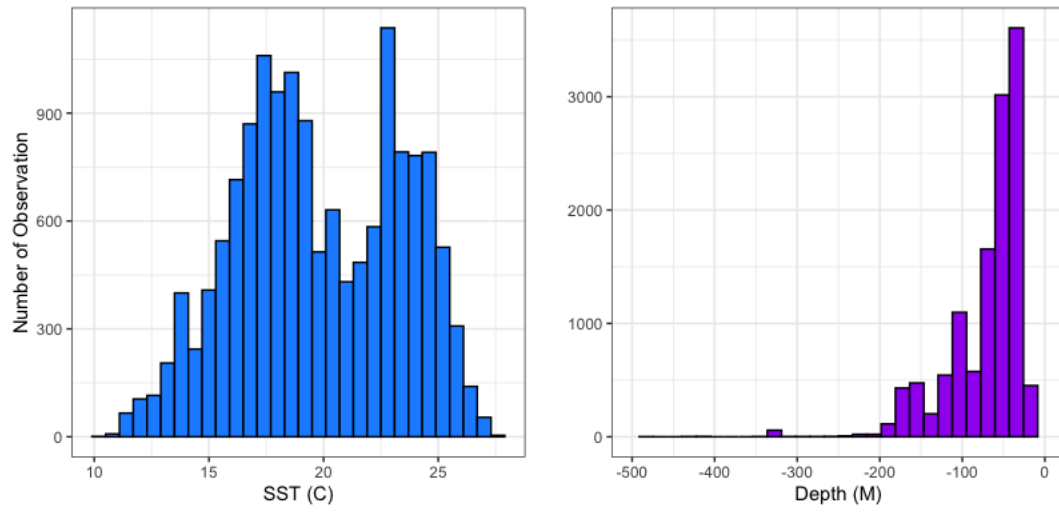


Figure 2. Distribution of local covariates, sea surface temperature (SST) and depth, explored in VAST models examining the spatio-temporal dynamics of Atlantic bluefin tuna.

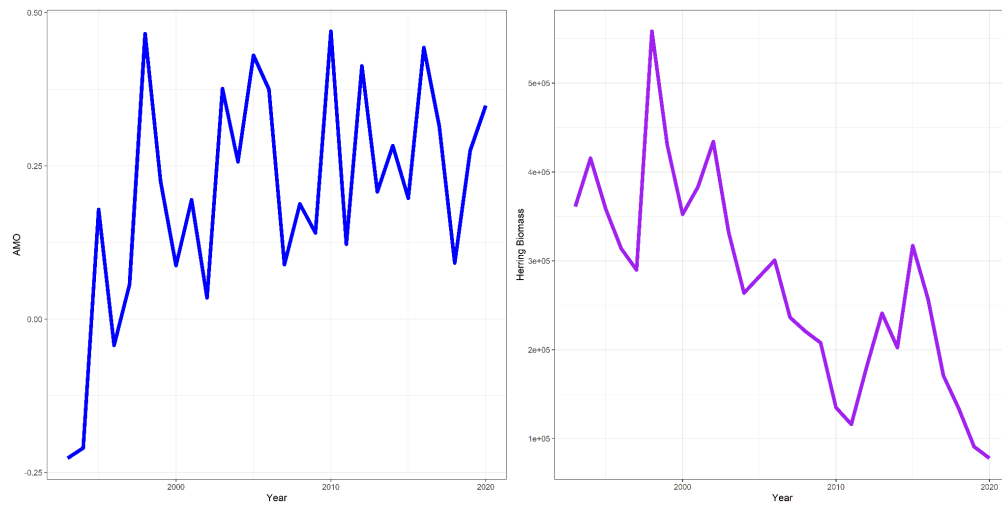


Figure 3. Regional time series explored in VAST models examining the spatio-temporal dynamics of Atlantic bluefin tuna.

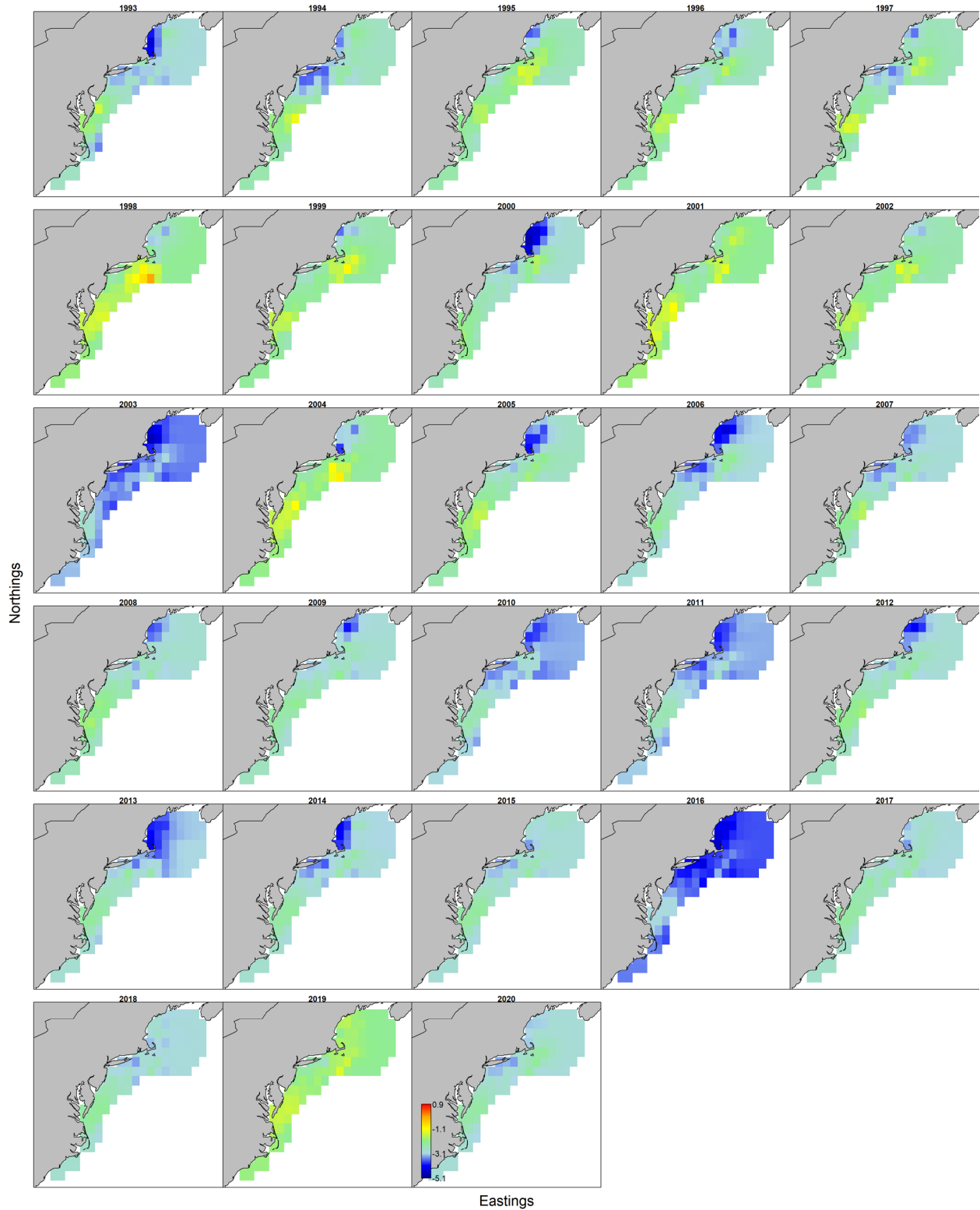


Figure 4: For large Atlantic Bluefin tuna, log density estimates from VAST model fit with all covariates (SST, AMO, herring abundance).

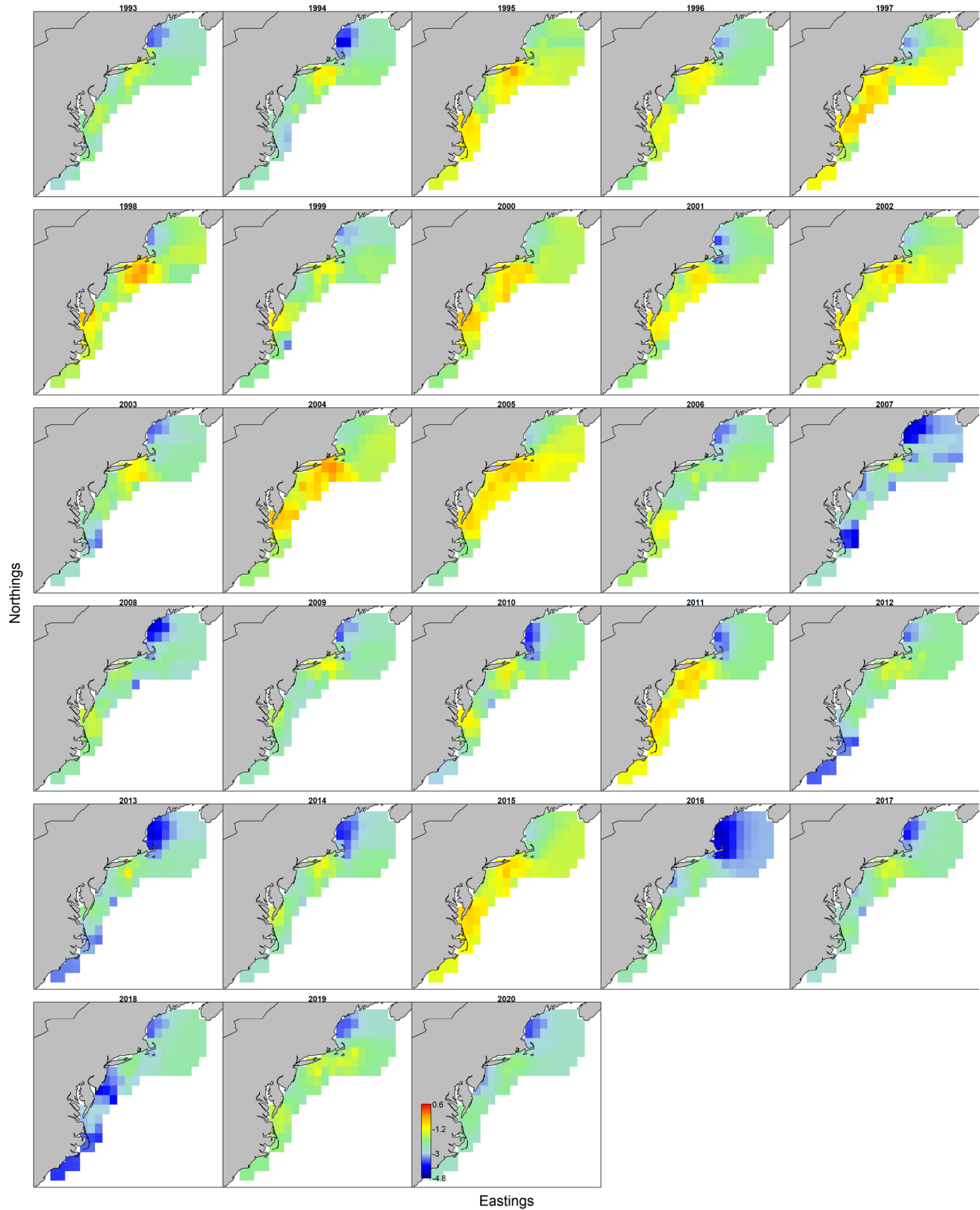


Figure 5: For small Atlantic Bluefin tuna, log density estimates from VAST model fit Gaussian Markov random fields and all covariates (SST, AMO, herring abundance).

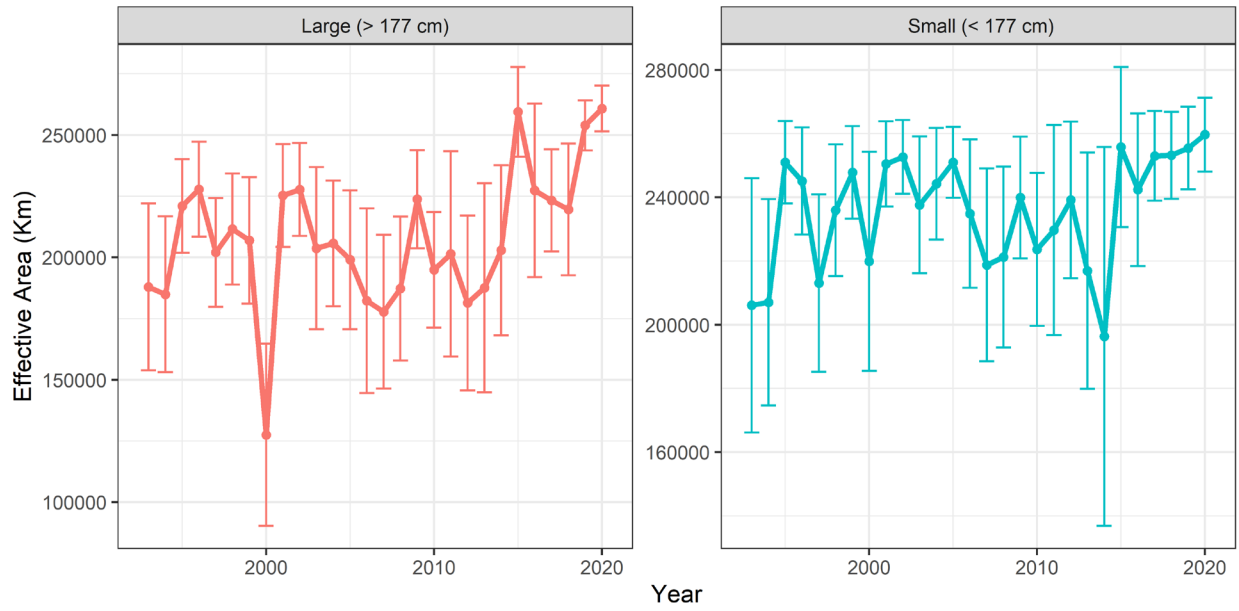


Figure 6. VAST effective area occupied estimates for large and small Atlantic Bluefin tuna. The model is fit with Gaussian Markov random fields and all covariates (SST, AMO, herring abundance).

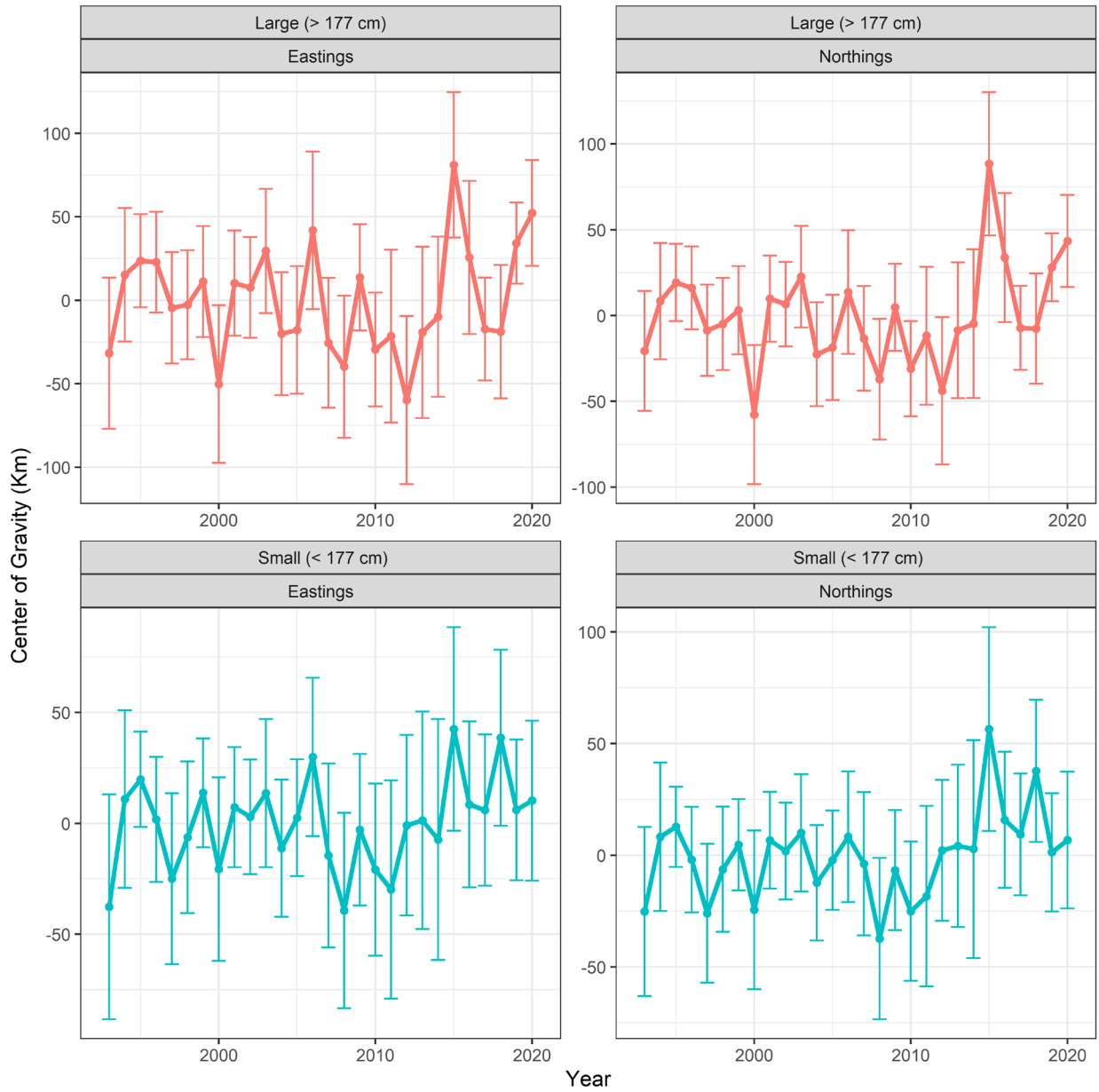


Figure 7. VAST spatial distribution changes estimates for large and small Atlantic bluefin tuna. The model is fit with Gaussian Markov random fields and all covariates (SST, AMO, herring abundance).

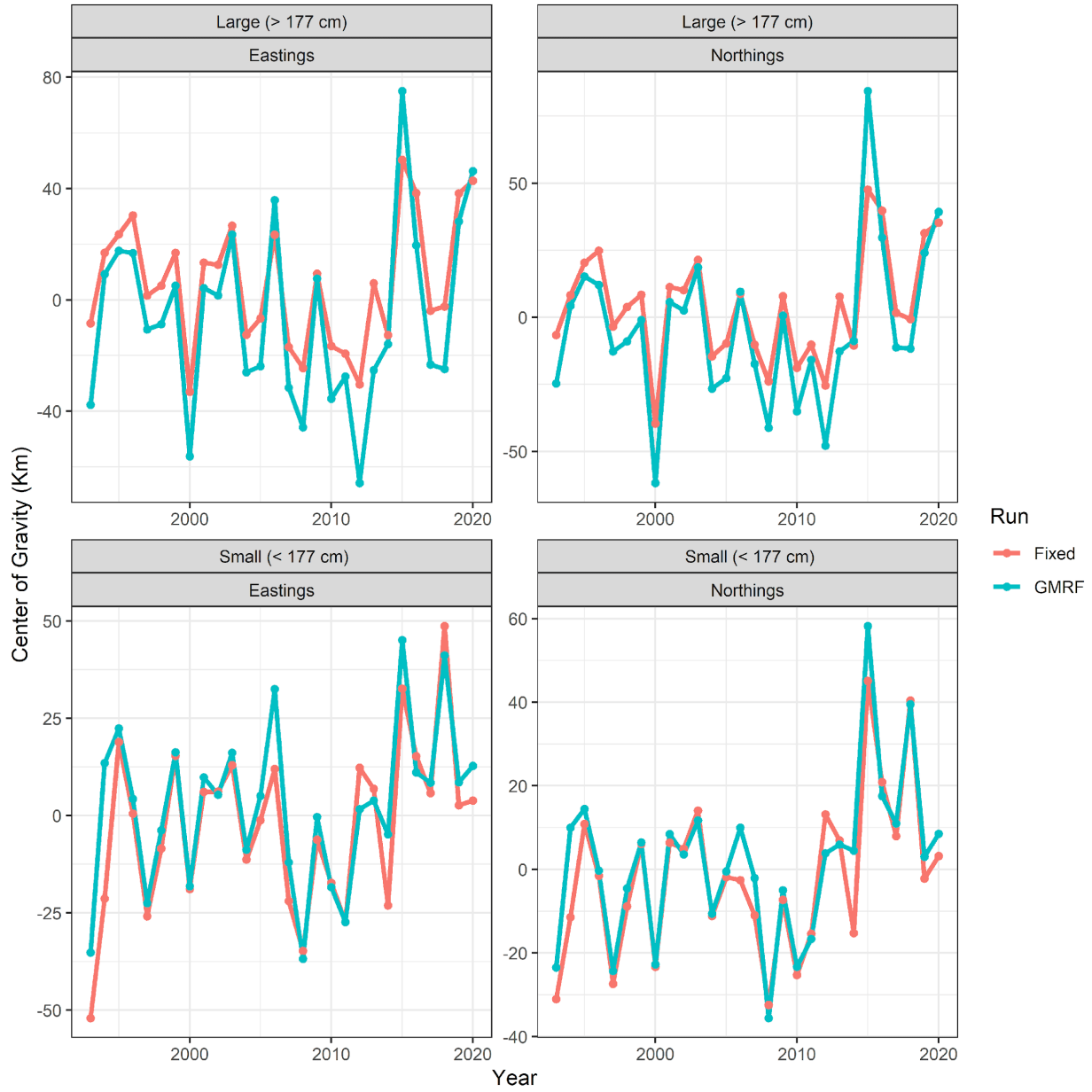


Figure 8. Counterfactual analysis exploring if covariates can explain observed distribution shifts. Blue represents VAST model runs used to estimate distribution shifts and fit with the Gaussian Markov random fields (GMRF), while red is the model run with only covariates (fixed effects).

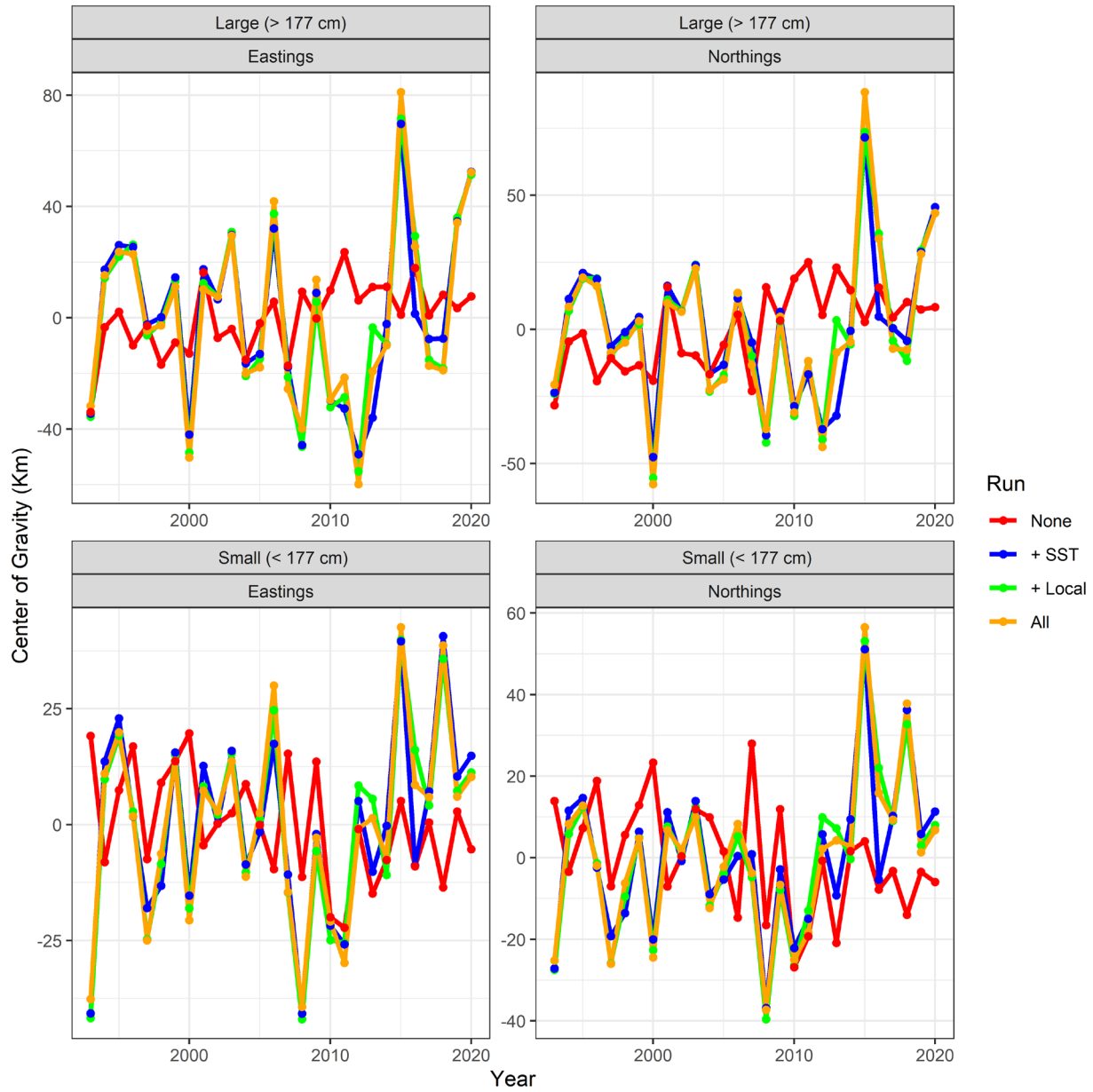


Figure 9. Counterfactual analysis sensitivity runs. Red is a VAST model without Gaussian Markov random fields (GMRF) and covariates. Following model runs continuously add covariates, blues adds sea surface temperature (SST), green adds local covariates (SST and depth), orange adds local and regional (AMO and herring abundance) covariates.

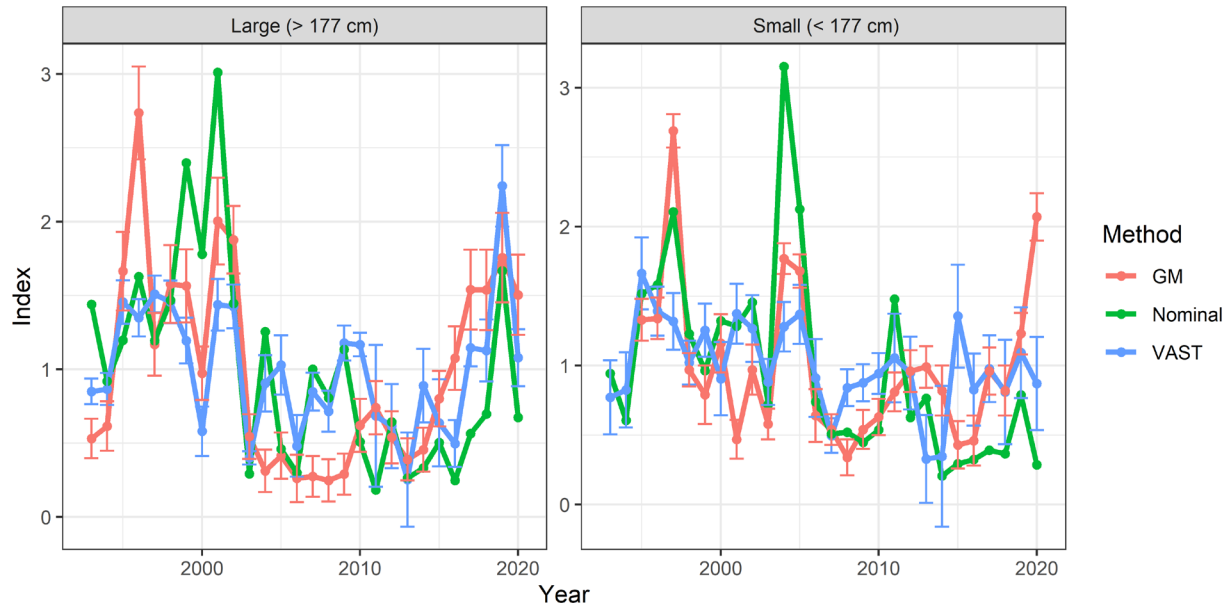


Figure 10. For Atlantic bluefin tuna, standardized indices of abundance from previous generalized models (GM) and the spatio-temporal VAST model. Error bars are +/- two standard error. The VAST model includes SST as an effect on density.